Dynamics of Reaction of (*meso*-Tetrakis(2,6-dimethyl-3-sulfonatophenyl)porphinato)-iron(III) Hydrate with *tert*-Butyl Hydroperoxide in Aqueous Solution. 2. Establishment of a Mechanism That Involves Homolytic O–O Bond Breaking and One-Electron Oxidation of the Iron(III) Porphyrin

P. N. Balasubramanian,[†] John R. Lindsay Smith,[‡] Michael J. Davies,[‡] Thomas W. Kaaret,[†] and Thomas C. Bruice*,[†]

Contribution from the Department of Chemistry, University of California at Santa Barbara, Santa Barbara, California 93106. *Received July 5, 1988*

Abstract: The reaction of *t*-BuOOH with the water soluble and non-μ-oxo dimer forming (5,10,15,20-tetrakis(2,6-dimethyl-3-sulfonatophenyl)porphinato)iron(III) hydrate ((**1**)$Fe^{III}(X)(H_2O)$ where X = H_2O or HO^-) was studied in aqueous solution between pH 2 and 13 in the absence of an agent for the trapping of reaction intermediates. Products of *t*-BuOOH decomposition are $(CH_3)_2CO$ (90%), CH_3OH (90%), and *t*-BuOH (15%), while neither CH_4, C_2H_6, O_2, nor $(t\text{-BuO})_2$ could be detected. That $(CH_3)_2CO$ and CH_3OH are formed through fragmentation of *t*-BuO$^\bullet$ to $(CH_3)_2CO$ and $CH_3^\bullet$ is shown by the observation that the reaction of $Ph(CH_3)_2COOH$ with (**1**)$Fe^{III}(X)(H_2O)$ provides acetophenone but not phenol. This must be a consequence of homolytic O–O bond scission with the formation of $Ph(CH_3)_2CO^\bullet$. The reaction of (**1**)$Fe^{III}(X)(H_2O)$ with *m*-$ClC_6H_4CO_3H$ and the hydroperoxides *t*-BuOOH, $Ph(CH_3)_2COOH$, $Ph_2C(CO_2CH_3)OOH$, and $Ph_2C(CN)OOH$ between pH 5 and 7 leads to the buildup of (**1**)$Fe^{IV}(X)(H_2O)$ species. The formation of an iron(IV)–oxo porphyrin species was established by titrimetric experiments as well as by carbon microelectrode voltommetry and $1e^-$ spectroelectrochemical generation of authentic (**1**)$Fe^{IV}(X)(H_2O)$ species. Formation of (**1**)$Fe^{IV}(X)(H_2O)$ species on oxidation of (**1**)$Fe^{III}(X)(H_2O)$ with *m*-$ClC_6H_4CO_3H$ occurs in the absence of O_2, while formation of (**1**)$Fe^{IV}(X)(H_2O)$ species on oxidation of (**1**)$Fe^{III}(X)(H_2O)$ by the alkyl hydroperoxides, *t*-BuOOH and $Ph(CH_3)_2COOH$, requires the presence of O_2. These observations require for the peracid a $2e^-$ oxidation with heterolytic O–O bond cleavage [*m*-$ClC_6H_4CO_3H$ + (**1**)$Fe^{III}(X)(H_2O)$ → *m*-$ClC_6H_4CO_2H$ + ($^{+\bullet}$**1**)$Fe^{IV}(X)(H_2O)$] followed by a comproportionation reaction [(**1**)$Fe^{III}(X)(H_2O)$ + ($^{+\bullet}$**1**)$Fe^{IV}(X)(H_2O)$ → 2(**1**)$Fe^{IV}(X)(H_2O)$], while in the case of the reaction of the alkyl hydroperoxides a $1e^-$ oxidation occurs with homolytic O–O bond breaking. The fragmentation of the resultant *t*-BuO$^\bullet$ provides $(CH_3)_2CO$ and $CH_3^\bullet$, and reaction of the latter with (**1**)$Fe^{III}(X)(H_2O)$ yields CH_3OH and (**1**)$Fe^{II}(X)(H_2O)$. The resultant iron(II) porphyrin species reacts with O_2 [2(**1**)$Fe^{II}(X)(H_2O)$ + O_2 → 2(**1**)$Fe^{IV}(X)(H_2O)$]. The putative (**1**)$Fe^{II}(X)(H_2O)$ intermediate was identified by its trapping with CO. Also, *t*-BuO$^\bullet$ and $CH_3^\bullet$ intermediates were identified by their spin trapping with 5,5-dimethyl-1-pyrroline *N*-oxide. The rate constant for reaction of hydrogen peroxide with (**1**)$Fe^{IV}(X)(H_2O)$ exceeds that for other hydroperoxides investigated. Thus, (**1**)$Fe^{IV}(X)(H_2O)$ does not accumulate in the reaction of H_2O_2 with (**1**)$Fe^{III}(X)(H_2O)$. The rapid reaction of H_2O_2 with (**1**)$Fe^{IV}(X)(H_2O)$ provides (**1**)$Fe^{III}(X)(H_2O)$ and presumably $O_2^{\bullet-}$ + H^+. This marks the first observation of the reaction of H_2O_2 with a compound II species. The pH dependence of the kinetics for the reaction of (**1**)$Fe^{III}(X)(H_2O)$ with *t*-BuOOH has been determined and shown to be comparable to those of a previous study which employed 2,2′-azinobis(3-ethylbenzthiozolinesulfonate) (ABTS) as a trap for reactive intermediates. The previous investigation allowed the identification of the four critical complexes whose decompositions are the commitment steps in the catalysis. Therefore, the same commitment steps are involved in the absence of ABTS.

In a previous paper we presented a study of the reaction of *t*-BuOOH with (5,10,15,20-tetrakis(2,6-dimethyl-3-sulfonatophenyl)porphinato)iron(III) hydrate ((**1**)$Fe^{III}(X)(H_2O)$ where X = H_2O or HO^-) in aqueous solution between pH 2 and 13 using 2,2′-azinobis(3-ethylbenzthiozolinesulfonate) (ABTS) as a trap for intermediate oxidizing species.[1] The important conclusions were as follows: (i) the reaction is first order in both *t*-BuOOH and (**1**)$Fe^{III}(X)(H_2O)$ and the second-order rate constant (k_{Iy}) exhibits a complex dependence upon pH; (ii) complexing of *t*-BuOOH by (**1**)$Fe^{III}(X)(H_2O)$ precedes oxidation of the iron(III) porphyrin and the proton ionizations (**1**)$Fe^{III}(OH_2)$(*t*-BuOOH) → H^+ + (**1**)$Fe^{III}(OH_2)$(*t*-$BuOO^-$) and (**1**)$Fe^{III}(OH)$(*t*-BuOOH) → H^+ + (**1**)$Fe^{III}(OH)$(*t*-$BuOO^-$) are important in the determination of the dependence of k_{Iy} on pH; (iii) the products of the reaction are those expected from a reaction involving a homolytic decomposition of *t*-BuOOH; (iv) the reaction of *t*-BuOOH with (**1**)$Fe^{III}(X)$ is not subject to general-acid or general-base catalysis at any pH value; and (v) neither the polar nor steric effects of the hydroperoxide moieties are important in the determination of k_{Iy}.[2,3] Two kinetically competent homolytic mechanisms, consistent with the products, were considered. The first involves homolysis of the hydroperoxide O–O bond to provide (**1**)$Fe^{IV}(X)(OH)$ + $(CH_3)_3C\text{-}O^\bullet$ as primary products, while the second mechanism involves the initial formation of (**1**)$Fe^{II}(X)$ + $(CH_3)_3COO^\bullet$.

We report now a study of the reaction of *t*-BuOOH with (**1**)$Fe^{III}(X)(H_2O)$ in the absence of ABTS trapping agent and in the presence and absence of O_2 and CO. The study involves kinetics and product analysis, the observation of iron(IV) and some iron(II) porphyrin intermediate, and EPR identification of radical intermediates.

Experimental Section

Much of the experimental procedures used in this study have been described previously.[1] Buffer solutions were prepared from reagent-grade chloroacetic acid (Aldrich, Matheson Collman Chemicals), sodium borate, sodium carbonate, and sodium phosphates (NaH_2PO_4, Na_2HPO_4) and were made free of heavy-metal impurities as given previously.[4] Carbon monoxide (Linde, technical grade) was used as received. Sodium dithionite was purchased from Baker and Adamson Chemicals. 5,5-

[†] Department of Chemistry, University of California at Santa Barbara.
[‡] Department of Chemistry, University of York, York, England.

(1) Lindsay, Smith, J. R.; Balasubramanian, P. N.; Bruice, T. C. *J. Am. Chem. Soc.* **1988**, *110*, 7411.
(2) (a) Lee, W. A.; Bruice, T. C. *J. Am. Chem. Soc.* **1985**, *107*, 513. (b) Lee, W. A.; Yuan, L.-C.; Bruice, T. C. *J. Am. Chem. Soc.* **1988**, *110*, 4277.
(3) Bruice, T. C.; Balasubramanian, P. N.; Lee, R. W.; Lindsay Smith, J. R. *J. Am. Chem. Soc.* **1988**, *110*, 7890.
(4) (a) Zipplies, M. F.; Lee, W. A.; Bruice, T. C. *J. Am. Chem. Soc.* **1986**, *108*, 4433. (b) Balasubramanian, P. N.; Schmidt, E. S.; Bruice, T. C. *J. Am. Chem. Soc.* **1987**, *109*, 7865.

0002-7863/89/1511-1477$01.50/0

Dimethyl-1-pyrroline N-oxide (DMPO) was purified, before use, as described elsewhere.[5]

The kinetics of the reaction were studied in thermostated cell holders (30 °C) by using both a Perkin-Elmer Model 553 fast-scan spectrophotometer and a Cary 14 spectrophotometer interfaced to a Zenith computer equipped with data acquisition and processing software (On-Line Instruments Systems, Inc.). A rapid-scan stopped-flow spectrophotometer (housed inside a N_2-filled glovebox) using the Harrick monochromator (Harrick Scientific, Ossining, NY) interfaced to an OLIS computer was used to follow the spectral changes of rapid reactions.

Experiments with carbon monoxide (CO) were carried out either by using argon atmospheres and Thunberg cuvettes or with regular cuvettes inside a N_2-filled glovebox which housed the spectrophotometer. Thunberg experiments were carried out to determine the spectral properties of (**1**)$Fe^{II}(H_2O)(CO)$. In a typical experiment, solutions of (**1**)$Fe^{III}(X)(H_2O)$ (4.69×10^{-6} M), buffered at pH 6.7, and sodium dithionite (0.04 M) were completely degassed with oxygen-free argon prior to mixing in Thunberg cuvettes. Mixing of the two solutions generates (**1**)$Fe^{II}(X)(H_2O)$ quantitatively.[6] Immediately after the formation of (**1**)$Fe^{II}(X)(H_2O)$, saturation of the solution with CO results in the appearance of the spectrum of the carbon monoxide adduct ((**1**)$Fe^{II}(H_2O)(CO)$). In the other experiment, a solution of (**1**)$Fe^{III}(X)(H_2O)$, buffered at pH 6.77, was prepared inside the N_2-filled glovebox. The cuvette was capped with a rubber septum provided with inlet and outlet ports and saturated with CO. There was then added *t*-BuOOH (to 6.0×10^{-5} M), and the reaction was followed by visible spectral repetitive scanning.

Spin-Trapping Experiments. EPR spin-trapping experiments were carried out with air-saturated solutions (22 °C) of DMPO. Spectra were recorded 2 min after mixing of reagents (and sequentially scanned in time-course experiments) with a Brucker ESP 300 spectrometer equipped with 100-kHz modulation and a Brucker ER035M gaussmeter for field calibration. Assignment of spectral lines was carried out as previously.[7]

Electrochemical Experiments. A Bioanalytical Systems (BAS) CV-27 voltammograph three-electrode potentiostat was used for linear sweep voltammetry and controlled-potential electrolysis experiments. Voltammograms were recorded on a Houston Instruments Model 100 x–y recorder. A 5-μm-diameter carbon fiber disk microelectrode was used as the working electrode for voltammetric experiments. For controlled-potential electrolysis a platinum-mesh working electrode was employed. All electrochemical cells were equipped with a platinum-flag auxiliary electrode, separated from the main compartment by a medium glass frit, and a Ag/AgCl reference electrode filled with aqueous tetramethylammonium chloride that was adjusted to 0.00 V vs SCE. All potentials reported are V vs SCE. Spectroelectrochemical spectra were recorded on a Cary 118 spectrophotometer.

Prior to each experiment the working electrode was pretreated in 1.0 M $HClO_4$ by stepping five to seven times between 0.00 and 1.20 or 0.00 and −0.85 V for cathodic and anodic measurements, respectively. The electrode was then throughly rinsed with the appropriate buffer solution and dried.

Results

The pseudo-first-order rate constants (k_{obsd}) for the reaction of *tert*-butyl hydroperoxide (*t*-BuOOH) with (5,10,15,20-tetrakis(2,6-dimethyl-3-sulfonatophenyl)porphinato)iron(III) hydrate ((**1**)$Fe^{III}(H_2O)(X)$; where X = H_2O or HO^-) have been determined in aqueous solution by monitoring spectrally the disappearance of the iron(III) Soret band at constant values of pH (30 °C, μ = 0.22 with $NaNO_3$, under aerobic conditions unless otherwise specified). At certain pH values intermediate porphyrin species have been observed. EPR spin-trap studies have been carried out to identify and follow the time course of the formation of *t*-BuOOH-derived radical species. The ultimate products formed from the radical intermediates have been determined.

The products that arise from the decomposition of *t*-BuOOH catalyzed by (1)$Fe^{III}(X)(H_2O)$ were determined at termination of the reactions by direct GC analysis using standard curves for quantitation. At pH 6.77 with $[t\text{-BuOOH}]_i = 1.2 \times 10^{-3}$ M and $[(\mathbf{1})Fe^{III}(X)(H_2O)]_i = 1.4 \times 10^{-5}$ M, products are $(CH_3)_2CO$ (90%), CH_3OH (90%), and *t*-BuOH (15%).[1] With $[t\text{-BuOOH}]_i = 3.0 \times 10^{-5}$ M and $[(\mathbf{1})Fe^{III}(X)(H_2O)]_i = 4.6 \times 10^{-6}$ M, assays for $(CH_3)_2CO$ at pH values 7.3, 8.5, 10.6, and 11.2 showed ~90% yields. In the latter experiments the $[t\text{-BuOOH}]_i$ is too low to assay for CH_3OH. From reactions carried out in sealed vials under argon, GC–MS analysis of the argon head space showed that neither CH_4 nor C_2H_6 was formed. Reactions were carried out in a sealed reaction chamber with an O_2 electrode at pH 6.7, using the same concentration of reagents as employed for the GC studies. No oxygen could be detected as a product. In the many GC analyses carried out in the course of this study $(t\text{-BuOH})_2$ was never detected.

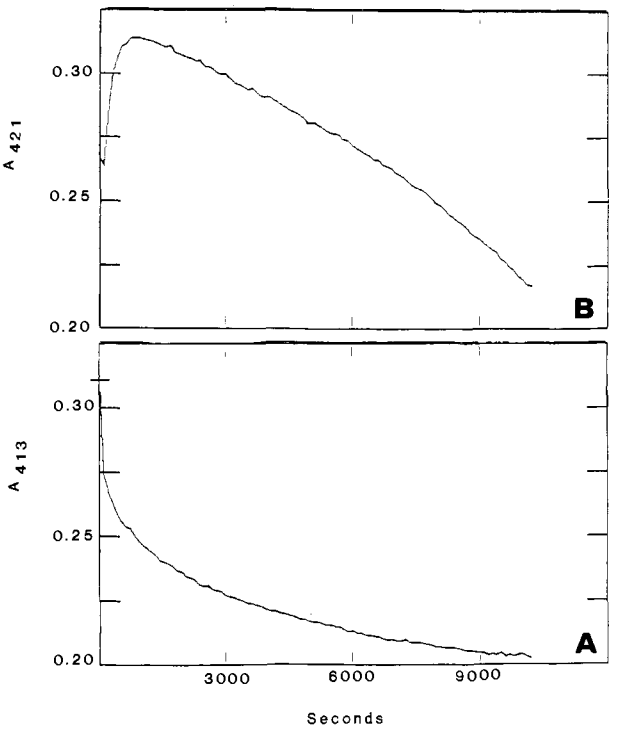

Figure 1. Plot of the changes in absorbance vs time for the reaction of $[t\text{-BuOOH}]_i$ (3.0×10^{-5} M) with $[(\mathbf{1})Fe^{III}(H_2O)(X)] = 4.6 \times 10^{-6}$ M, (50 mM phosphate buffer, pH 6.77, μ = 0.22 with $NaNO_3$) at 30 °C. Panel A corresponds to the changes in absorbance at 413 nm, and B corresponds to the changes in absorbance at 421 nm.

Product analysis for the reaction of cumyl hydroperoxide (9.7×10^{-4} M) with (1)$Fe^{III}(X)(H_2O)$ (5.3×10^{-5} M) was carried out at four different pH values (2.19, 6.77, 10.31, and 13.0). By GC, $(CH_3)_2C{=}O$ is not a product. HPLC analyses with a reverse-phase column (All Tech/Applied Science 250 × 4.6 mm column packed with Lichrosorb RP-18 5 μm) using MeOH/H_2O (50% v/v) as solvent showed acetophenone in >90% yield at pH 6.77, whereas at pH values 2.19, 10.31, and 13.0, the yields of acetophenone were 62%, 71%, and 59%, respectively. Phenol could not be detected as a product in any of the reactions.

The Reaction of (1)$Fe^{III}(X)(H_2O)$ with *t*-BuOOH between pH 5 and 7 Gives Rise To Observable Hypervalent Iron–Oxo Porphyrin Intermediates. With a 7-fold excess of *t*-BuOOH over (**1**)$Fe^{III}(X)(H_2O)$ (4.63×10^{-6} M) at pH 6.7 ($[Na_2HPO_4/NaH_2PO_4]_T$ = 0.068 M), initiation is accompanied by a biphasic decrease (both phases being pseudo first order) in the Soret band (413 nm) of (**1**)$Fe^{III}(X)(H_2O)$ (Figure 1A). As (**1**)$Fe^{III}(X)(H_2O)$ disappears, there is observed, after a lag phase, the formation of an intermediate absorbing at 421 nm. Once A_{421} reaches a maximum it decreases with the reappearance of (**1**)$Fe^{III}(X)(H_2O)$ (A_{413}) (Figure 1B). Observation of a lag phase in the formation of the 421-nm-absorbing species shows that this species is not formed directly on reaction of *t*-BuOOH with (**1**)$Fe^{III}(X)(H_2O)$. During the course of the reaction, which involves seven turnovers of iron porphyrin, there is seen a 15% loss of $[(\mathbf{1})Fe^{III}(X)(H_2O)]$ (Figure 2). At higher concentrations of *t*-BuOOH the species absorbing at 421 nm appears without a lag phase. With a 10-fold excess of *t*-BuOOH, there is seen a 20% loss of [(**1**)Fe^{III}-

(5) Beuttner, G. R.; Oberley, L. W. *Biochem. Biophys. Res. Commun.* **1978**, *83*, 69.

(6) (a) Geibel, J.; Cannon, J.; Campbell, D.; Traylor, T. G. *J. Am. Chem. Soc.* **1978**, *100*, 3575. (b) Traylor, T. G.; White, D. K.; Campbell, D. H.; Berzinis, A. P. *J. Am. Chem. Soc.* **1981**, *103*, 4932. (c) Traylor, T. G.; Koga, N.; Deardurff, L. A.; *J. Am. Chem. Soc.* **1985**, *107*, 6504.

(7) Davies, M. J. *Biochim. Biophys. Acta* **1988**, *964*, 28.

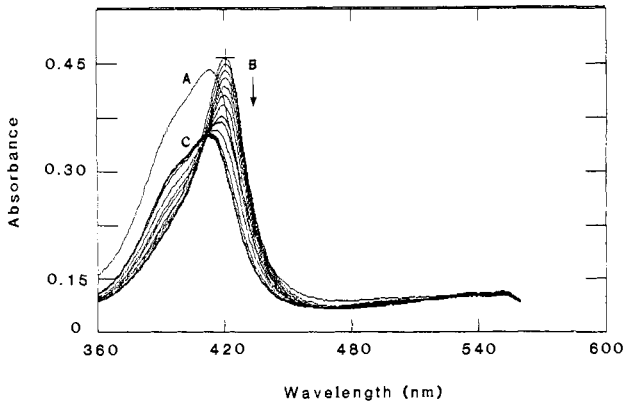

Figure 2. Repetitive scanning of a reaction mixture of (**1**)$Fe^{III}(H_2O)(X)$ (4.6×10^{-6} M) with $[t\text{-BuOOH}]_i = 3.0 \times 10^{-5}$ M, at pH 6.7 (50 mM phosphate buffer, $\mu = 0.22$ with $NaNO_3$, 30 °C). Spectrum A corresponds to that of (**1**)$Fe^{III}(H_2O)(X)$ before addition of *t*-BuOOH. B is a series of consecutive scans at various time intervals showing the formation and decay of intermediate species with a $\lambda_{max} = 421$ nm, and C is the final spectrum of the regenerated (**1**)$Fe^{III}(H_2O)(X)$.

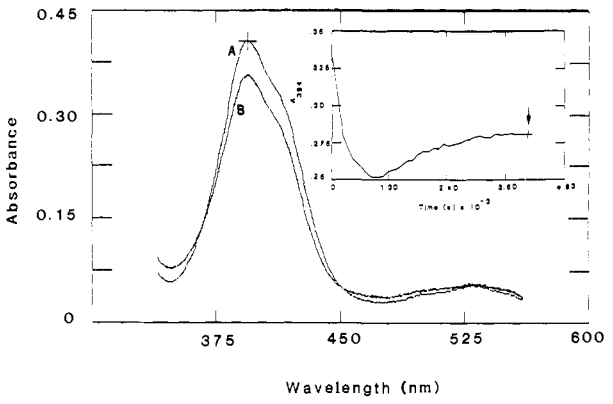

Figure 3. Curve A corresponds to the spectrum of (**1**)$Fe^{III}(H_2O)_2$ (4.6×10^{-6} M) at pH 5.14, and curve B corresponds to the spectrum of iron(IV) species formed at pH 5.14 upon completion of reaction with $[t\text{-BuOOH}]_i$ (3.0×10^{-5} M). Inset: Plot of the change in absorbance at 394 nm vs time for the reaction of (**1**)$Fe^{III}(H_2O)_2$ (4.6×10^{-6} M) with $[t\text{-BuOOH}]_i$ (3.0×10^{-5} M) at pH 5.14 (50 mM acetate buffer, $\mu = 0.22$ with $NaNO_3$, 30 °C).

$(X)(H_2O)]$. With an 80-fold excess of the *t*-BuOOH over $[(\mathbf{1})Fe^{III}(X)(H_2O)]_i$, the loss is 44%, etc.

Observation of the 421-nm-absorbing species is possible only when its rate of formation is somewhat greater than its rate of disappearance. Spectrophotometric titration by addition of small aliquots of a *t*-BuOOH solution to one of (**1**)$Fe^{III}(X)(H_2O)$ (4.6×10^{-6} M) shows that nearly 2.5 equiv of *t*-BuOOH is required to observe a peak absorbance at 421 nm. At just sufficient [*t*-BuOOH], formation of A_{421} is preceded by a lag phase. Addition of ABTS [$(8.3\text{–}32.0) \times 10^{-5}$ M] at the time of maximum formation of A_{421} provides nearly 1.9 equiv of $ABTS^{\bullet+}$ based on $[(\mathbf{1})Fe^{III}(X)(H_2O)]_i$. Of these, 0.6 arises instantly and the remaining 1.3 equiv are formed with the pseudo-first-order rate constant of $(4.2 \pm 0.4) \times 10^{-3}$ s^{-1}. Thus, 0.6 equiv of the initial (**1**)$Fe^{III}(X)(H_2O)$ has been converted to the intermediate, which reacts instantly with ABTS to provide $ABTS^{\bullet+}$ plus (**1**)$Fe^{III}(X)(H_2O)$. The remaining $ABTS^{\bullet+}$ arises from turnover of the catalyst in reacting with unreacted *t*-BuOOH. As expected, the latter formation of $ABTS^{\bullet+}$ is associated with a rate constant identical with that seen when starting with *t*-BuOOH and (**1**)$Fe^{III}(X)(H_2O)$ in solution with ABTS present.[1] By knowing A_{421} at the time of addition of ABTS, the spectral properties of the intermediate can be determined as approximately λ_{max} 421 nm [ϵ_{max} $(1.3 \pm 0.1) \times 10^5$ M^{-1} cm^{-1}].

The half-wave potentials (V vs SCE) for the oxidation and reduction of (**1**)$Fe^{III}(X)(H_2O)$ in water were determined at a carbon microelectrode by linear sweep voltammetry (eq 1). Under

$$(\mathbf{1})Fe^{II}(X)(H_2O) \underset{\text{pH 5.14}}{\overset{\text{pH 6.75}}{\xrightarrow[-0.13]{-1e^-,\ -0.19}}} (\mathbf{1})Fe^{III}(X)(H_2O) \xrightarrow[0.86]{-1e^-,\ 0.81} (\mathbf{1})Fe^{IV}(X)(H_2O) \quad (1)$$

the steady-state conditions employed, sigmomoidal-shaped voltammograms are obtained for both oxidative and reductive processes. Based on the comparison of ratio of the peak currents (0.9 for oxidation/reduction) for oxidation and reduction of the iron(III) species (eq 1), an assignment of a $1e^-$ process is made for the oxidation of (**1**)$Fe^{III}(X)(H_2O)$. Spectroelectrochemical oxidations of (**1**)$Fe^{III}(X)(H_2O)$ at 0.93 V (pH 6.75) produces a (**1**)$Fe^{IV}(O)(X)$ species whose spectrum (λ_{max} 420 nm) is virtually identical with that obtained with *t*-BuOOH as oxidant at the same pH.

The reaction of a 7-fold excess of *t*-BuOOH with (**1**)$Fe^{III}(X)(H_2O)$ was also examined at pH 5.14. The absorbance at 394 nm (Soret band position for (**1**)$Fe^{III}(X)(H_2O)$ at this pH) first decreases rapidly and then increases with formation of a quite stable higher valent iron–oxo porphyrin species. The overall conversion of (**1**)$Fe^{III}(X)(H_2O)$ to the final species is quantitative (vide infra). This product possesses the same λ_{max} as (**1**)$Fe^{III}(X)(H_2O)$ but an ϵ_{max} ~30% less than that of (**1**)$Fe^{III}(X)(H_2O)$ (Figure 3). The increase in absorbance accompanying the formation of the second product is associated with isosbestic points at 446 and 364 nm. Addition of about a 20-fold excess of ABTS (8.3×10^{-5} M), at some time after the formation of the stable product was complete (Figure 3 inset), provided 1 equiv of $ABTS^{\bullet+}$ on the basis of $[(\mathbf{1})Fe^{III}(X)(H_2O)]_i$. Thus, the product formed at pH 5.14 is $1e^-$ oxidized above iron(III) porphyrin. The approximate spectral properties of this (**1**)$Fe^{IV}(O)(X)$ species is λ_{max} 394 nm [$\epsilon_{max} = (9.5 \pm 0.9) \times 10^4$ M^{-1} cm^{-1}].

Formation of the Intermediate Species (λ_{max} 421 nm) with Various Oxidants between pH 6 and 7. The reaction of (**1**)$Fe^{III}(X)(H_2O)$ (4.6×10^{-6} M) with *m*-chloroperbenzoic acid ([MCPBA] = 1.5×10^{-5} M), diphenylcyanomethyl hydroperoxide ([$Ph_2(CN)COOH$] = 2.5×10^{-5} M), diphenyl(carbomethoxy) hydroperoxide ([$Ph_2C(CO_2Me)OOH$] = 3×10^{-5} M), and cumyl hydroperoxide ([$Me_2C(Ph)OOH$] = 7.6×10^{-5} M) generates the λ_{max} 421 nm intermediate observed with the oxidant *t*-BuOOH. Stopped-flow rapid-scan spectrophotometry was employed to follow the reaction with MCPBA (Figure 4A–C). Inspection of Figure 4A shows that the disappearance of (**1**)$Fe^{III}(X)(H_2O)$ (413 nm) is accompanied by an increase followed by a decrease in A_{421} (Figure 4B) and an accompanying increase of A_{413} (Figure 4C). There is ~30% loss in $[(\mathbf{1})Fe^{III}(X)(H_2O)]$. The second-order rate constant for reaction of MCPBA with (**1**)$Fe^{III}(X)(H_2O)$ at pH 6.7 is ~10^6 M^{-1} s^{-1}.[3] That both the rate of formation and disappearance of the species absorbing at 421 nm are much greater than seen with *t*-BuOOH shows that the intermediate reacts with the oxidant.

The reaction of (**1**)$Fe^{III}(X)(H_2O)$ (4.6×10^{-6} M) with H_2O_2 (5.0×10^{-5} M) was studied at pH 6.75 by repetitive scanning of the spectrum of (**1**)$Fe^{III}(X)(H_2O)$ in the wavelength region of 700–340 nm. A 421-nm-absorbing species is not seen. There is only a continual decrease in the absorbance of (**1**)$Fe^{III}(X)(H_2O)$, until all the H_2O_2 is consumed and 44% of the (**1**)$Fe^{III}(X)(H_2O)$ is destroyed.

Another experiment was carried out to study the reaction of the 421-nm-absorbing species with H_2O_2. At pH 6.75, the 421-nm species was generated to its maximum ($[t\text{-BuOOH}] = 3.0 \times 10^{-5}$ M, $[(\mathbf{1})Fe^{III}(X)] = 4.6 \times 10^{-6}$ M) when H_2O_2 (3.3×10^{-5} M) was added. There was observed a relatively rapid decrease in A_{421}, and the spectrum of (**1**)$Fe^{III}(X)(H_2O)$ was regenerated slowly as in the reaction of *t*-BuOOH with (**1**)$Fe^{III}(X)(H_2O)$. The minimal second-order rate constant (126 M^{-1} s^{-1}) for the reaction of H_2O_2 with the 421-nm-absorbing species was calculated by the initial rate method.

The Question of Intermediate Formation on Reaction of *t*-BuOOH with (1)$Fe^{III}(X)(H_2O)$ at pH Values <5 and >7. Only a very small bathochromic shift in the Soret band (2–3 nm) accompanies the decrease in absorbance between 280 and 600 nm on reaction of *t*-BuOOH (3×10^{-5} M) with (**1**)$Fe^{III}(X)(H_2O)$

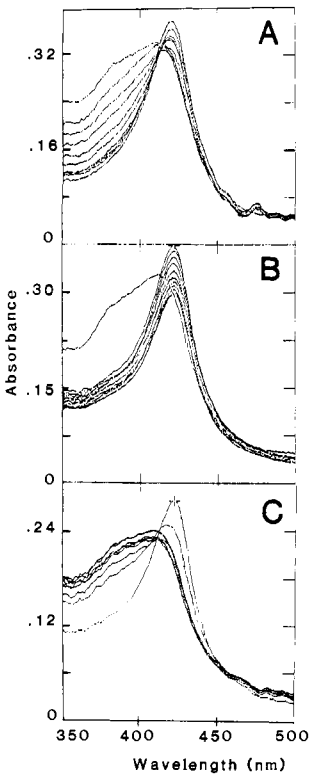

Figure 4. Rapid-scan stopped-flow reactions of (**1**)$Fe^{III}(H_2O)(X)$ with *m*-chloroperbenzoic acid at pH 6.7 (μ = 0.22 with $NaNO_3$, 30 °C). Panel A corresponds to the initial decrease in the absorbance at 413 nm and a simultaneous increase in absorbance at 421 nm, B corresponds to disappearance of the 421 nm species, and C corresponds to the regeneration of the spectrum of (**1**)$Fe^{III}(X)$ upon completion of the reaction.

(4.6×10^{-6} M) at pH values >7.0. In such experiments, a continuous biphasic decrease (20%) in absorbance in the region of the Soret band is observed until consumption of *t*-BuOOH is complete. At this time there is a very slow return of the position of the Soret band of (**1**)$Fe^{III}(X)(H_2O)$ but no increase in absorbance. The 20% decrease in absorbance is pH independent between pH 7.0 and 12.2 and is attributed to oxidative destruction of (**1**)$Fe^{III}(X)(H_2O)$. Between pH 2 and 5 (as in the experiments where pH >7.0), addition of *t*-BuOOH is accompanied by a continuous decrease in the Soret band of (**1**)$Fe^{III}(X)(H_2O)$ to a constant value which accounts for ~20% of (**1**)$Fe^{III}(X)(H_2O)$ destruction. There is no intervening shift of the Soret band from that of (**1**)$Fe^{III}(X)(H_2O)$. Again, there is no increase in absorbance on expenditure of all *t*-BuOOH.

Requirement of Oxygen for the Formation of 421-nm Intermediate Species. The reaction of (**1**)$Fe^{III}(X)(H_2O)$ (5.42×10^{-6} M) with *t*-BuOOH (6.0×10^{-5} M) was carried out under anaerobic conditions at pH 6.77. Addition of *t*-BuOOH resulted in the decrease of Soret maximum at 413 nm without a shift in the Soret maximum or an increase in absorbance at 421 nm. In the course of reaction, exposure of the reaction solution to bubbling oxygen provides the 421-nm-absorbing species. Thus, O_2 is required for the formation of the intermediate species with λ_{max} at 421 nm when *t*-BuOOH is used as oxidant.

The reaction of MCPBA (3.0×10^{-5} M) with (**1**)$Fe^{III}(H_2O)(X)$ (2.84×10^{-6} M) at pH 6.75 was followed under anaerobic conditions by use of a rapid-scan stopped-flow spectrophotometer. The disappearance of absorbance at 413 nm is accompanied by an increase in A_{421}. The same observation was also seen with MCPBA under aerobic conditions (vide supra). Thus, O_2 is not a requirement for the formation of the 421-nm-absorbing species with MCPBA. At pH 6.75 there is present in aqueous solution a mixture of (**1**)$Fe^{III}(H_2O)_2$ (λ_{max} 394 nm) and (**1**)$Fe^{III}(OH)(H_2O)$ (λ_{max} 413 nm). The disappearance of absorbance at 413 nm is complete at 5 ms. Decrease in absorbance of (**1**)$Fe^{III}(H_2O)(X)$ (394 nm) and increase in absorbance of the intermediate (421 nm) follow the pseudo-first-order rate law. Values of k_{obsd} are equal (80.0 ± 0.2 s^{-1}) when determined at either wavelength so that the second-order rate constant (k_{obsd}/[MCPBA]) under the nonturnover conditions equals 2.3×10^6 M^{-1} s^{-1}.[3]

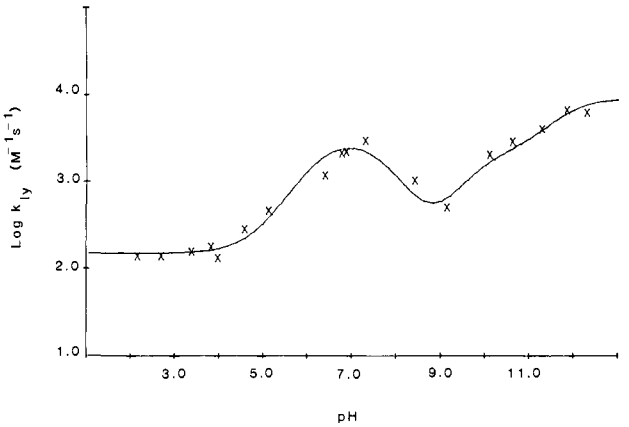

Figure 5. Plot of log of the second-order rate constant, k_2, for reaction of (**1**)$Fe^{III}(H_2O)(X)$ with *t*-BuOOH vs pH. ($[t\text{-BuOOH}]_i = 3.0 \times 10^{-5}$ M, $[(\mathbf{1})Fe^{III}(X)]_i = 4.6 \times 10^{-6}$ M, μ = 0.22 with $NaNO_3$, 30 °C.)

Table I. Comparison of the Values of the Kinetic Parameters Employed To Fit the log k_{ly} vs pH Profiles for the Reaction of *t*-BuOOH with (**1**)$Fe^{III}(X)(H_2O)$ in the Presence and Absence of ABTS Trap

equiv kinetic terms (eq 1)	values of determined constants		ratio without/with
	with ABTS	no ABTS	
k_a	43.0 M^{-1} s^{-1}	140 M^{-1} s^{-1}	3
k_b	1.20×10^3 M^{-1} s^{-1}	3.36×10^3 M^{-1} s^{-1}	3
k_c	8.57×10^2 M^{-1} s^{-1}	1.93×10^3 M^{-1} s^{-1}	2
k_d	2.14×10^3 M^{-1} s^{-1}	6.91×10^3 M^{-1} s^{-1}	3
pK_A	5.66	6.25	
pK_B	7.65	7.63	
pK_C	8.18	9.75	
pK_D	12.11	11.73	

Carbon Monoxide Trapping of (1)$Fe^{II}(X)(H_2O)$. Under anaerobic conditions, addition of *t*-BuOOH (6.0×10^{-5} M) to a carbon monoxide saturated solution of (**1**)$Fe^{III}(H_2O)(X)$ at pH 6.77 results in the shifting of Soret maximum from 413 nm to 417 nm with an increase in absorbance. With time the 417-nm absorbance decays to regenerate (**1**)$Fe^{III}(X)(H_2O)$. Also, sodium dithionite (0.04 M) reduction of (**1**)$Fe^{III}(H_2O)(X)$ (under argon, pH 6.77) results in the quantitative formation of (**1**)$Fe^{II}(H_2O)(X)$ (λ_{max} 430 nm, $\epsilon_{max} = 2.2 \times 10^5$ M^{-1} cm^{-1}), and saturation of the latter with CO generates (**1**)$Fe^{II}(X)(CO)$ (Soret maximum = 419 nm, $\epsilon_{max} = 2.5 \times 10^5$ M^{-1} cm^{-1}) instantaneously.[6] From these two experiments, which provide the ϵ_{max} for (**1**)$Fe^{II}(H_2O)(CO)$ and the observed ΔA_{417}, it can be calculated that the percentage of initial (**1**)$Fe^{III}(H_2O)(X)$ reacting with *t*-BuOOH to ultimately provide (**1**)$Fe^{II}(X)(CO)$ is 10%.

The pH dependence of the second-order rate constant (k_{ly}) for reaction of *t*-BuOOH with (1)$Fe^{III}(X)(H_2O)$ has been determined (Figure 5). The kinetic traces for the disappearance of (**1**)$Fe^{III}(H_2O)(X)$ are biphasic in the pH range 6–13 and below pH 5 the traces are reasonably good first-order reactions (loc cite). The value of $k_{ly} = k_{obsd}/[(\mathbf{1})Fe^{III}(X)(H_2O)]_i$ where k_{obsd} is taken as the pseudo-first-order rate constant for the first phase of (**1**)$Fe^{III}(X)(H_2O)$ disappearance (pH 6–13) or the pseudo-first-order rate constant for disappearance (below pH 5) of (**1**)$Fe^{III}(X)(H_2O)$. The points of Figure 5 are experimental and the line has been computer-generated from the empirical eq 2. The

$$k_{ly} = \underbrace{\frac{k_a a_H}{(K_A + a_H)}}_{(A)} + \underbrace{\frac{k_b K_A a_H}{(K_B K_A + K_A a_H + a_H^2)}}_{(B)} + \underbrace{\frac{k_c K_C}{(K_C + a_H)}}_{(C)} + \underbrace{\frac{k_d K_D}{(K_D + a_H)}}_{(D)} \quad (2)$$

Scheme I[a]

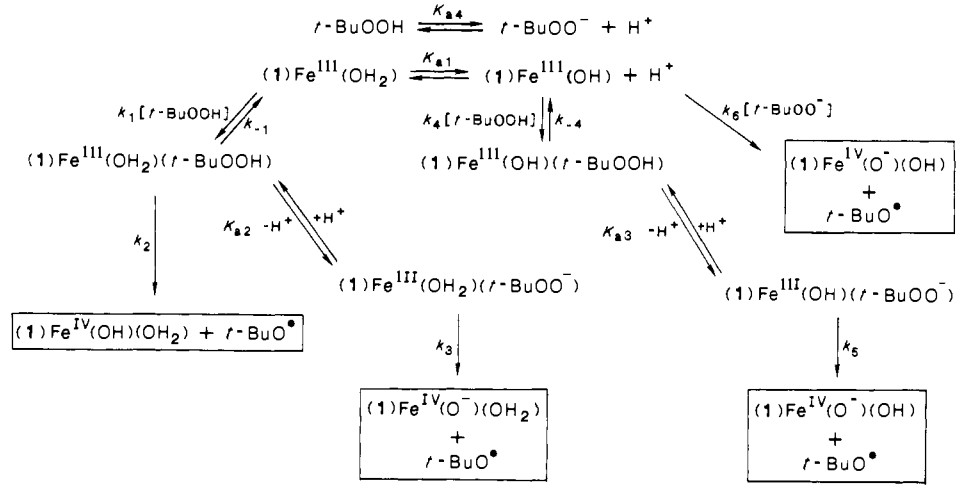

[a] The kinetic equivalents of the constants of Table I and the constants of this scheme are as follows: $k_a = k_1k_2/(k_{-1} + k_2)$; $k_b = k_1$; $k_c = k_4$; $k_d = k_6$; $pK_A = p(K_{a2}k_3/k_{-1})$; $pK_B = pK_{a1}$; $pK_C = p(K_{a3}k_5/k_{-4})$; and $pK_D = pK_{a4}$.

constants employed to fit the profile are included in Table I (see Discussion) for comparison to constants determined in experiments using ABTS as a trap (Scheme I).

The Spin Radical Trap 5,5-Dimethyl-1-pyrroline *N*-Oxide (DMPO) Has Been Employed To Monitor by EPR the Radical Species Formed in the Reaction of *t*-BuOOH with (1)Fe^{III}(X)(H_2O) (See Experimental Section). The radical species *t*-BuO•, *t*-BuOO•, and CH_3• could be identified at pHs 4.0, 6.0, 7.43, 9.0, and 10. The intensity of the spectral lines (signal height, SI, which is proportional to absolute concentration of radical adduct) for each radical adduct was determined as a function of time. The adduct concentrations are dependent on the efficiency of radical trapping by DMPO and on the stability of the trapped species toward further reaction; consequently, SI values are not necessarily equivalent to the relative concentrations of the species being trapped. From a representative plot (Figure 6) of SI vs time, from reaction of *t*-BuOOH (1.0×10^{-3} M) with (1)Fe^{III}(X)(H_2O) (2.0×10^{-5} M) at pH 10.0 (50 turnovers), it is seen that the SI for DMPO adducts of *t*-BuOO• and *t*-BuO• are comparable. The CH_3• adduct was also detected in low concentrations. The signal from the *t*-BuOO• adduct decays as a function of time. The rate of SI decay is dependent on both [(1)Fe^{III}(X)(H_2O)] (inversely) and pH, with slowest rates of decay being observed at pH 10 (with [(1)Fe^{III}(X)(H_2O)] = 2.0×10^{-6} M). An inverse dependence of SI for *t*-BuOO• adduct has been observed with other iron(III) porphyrins.[7] The SIs of the *t*-BuO• and CH_3• adducts increase as the reaction progresses, with this effect being most pronounced at low pH. At pH ≤7.43 an additional signal assigned to DMPOX, produced either by oxidation of the spin trap[8] or by decomposition of the *t*-BuO_2• adduct, is also observed; this species decays rapidly with time.

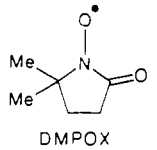

DMPOX

Discussion

The reaction of the non-μ-oxo dimer forming and nonaggregating (5,10,15,20-tetrakis(2,6-dimethyl-3-sulfonatophenyl)porphinato)iron(III) hydrate [(1)Fe^{III}(X)(H_2O), X = H_2O and HO^-] with *t*-BuOOH in aqueous solution (pH 2.2 and 13.0) provides $(CH_3)_2C{=}O$, CH_3OH, and *t*-BuOH. To the limits of detection neither O_2, (*t*-BuO)$_2$, CH_4, nor CH_3CH_3 are formed. The reaction is first order in [*t*-BuOOH]$_i$ and [(1)Fe^{III}(X)(H_2O)]$_i$.[1] In this study, as in the previous investigation using ABTS as a trap, the reaction of *t*-BuOOH with (1)Fe^{III}(X)(H_2O) is not subject to buffer catalysis. At pH 6.7 with [*t*-BuOOH] = 1.0×10^{-3} M the product yields are $(CH_3)_2C{=}O$ (90%), CH_3OH (90%), and *t*-BuOH (15%). With [*t*-BuOOH]$_i$ = 3.0×10^{-5} M, the yield of $(CH_3)_2C{=}O$ is ~90% at pH values 7.3, 8.5, 10.6, and 11.2. With increase of [ABTS] the yields of $(CH_3)_2C{=}O$ and *t*-BuOH approach 15% and 84%, respectively.[1] Comparison of products and their percent yields in the presence and absence of ABTS shows that 15% of *t*-BuOOH reacting with (1)Fe^{III}(X)(H_2O) provides intermediates that are not trapped by ABTS. This has been explained by the initial formation of solvent-caged intermediates (i.e., reactions that occur within the solvent cage are not subject to trapping while solvent-separated intermediates are subject to trapping[1]). The products formed through the solvent-caged species are $(CH_3)_2C{=}O$ and CH_3OH. The reactions of eq 3 were suggested. The ABTS-trapped intermediates would then be (1)-Fe^{IV}(O)(X) and *t*-BuO• (eq 4 and 5). The rate constant for

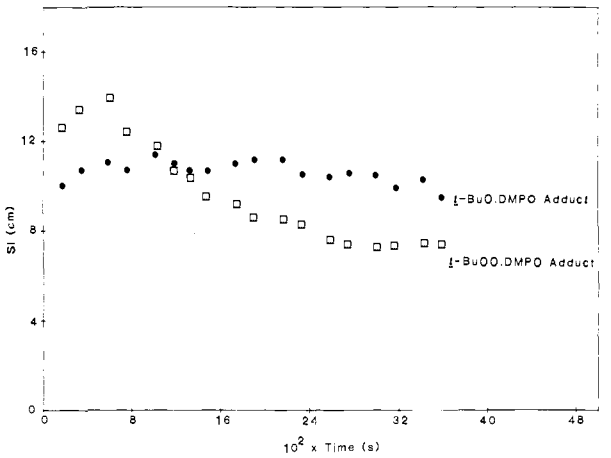

Figure 6. Plot of signal height intensity (SI) of various DMPO radical adducts vs time for the reaction of (1)Fe^{III}(H_2O)(X) (2.0×10^{-5} M) with *t*-BuOOH (1.0×10^{-3} M) at pH 9.95 ([DMPO]$_i$ = 5.0×10^{-2} M; μ = 0.22 with $NaNO_3$, 30 °C).

$$(1)Fe^{III}(X)(H_2O) + (CH_3)_3COOH \rightarrow [(1)Fe^{IV}(X)(OH)\ {}^{\bullet}OC(CH_3)_3]$$

$$[(1)Fe^{IV}(X)(OH)\ {}^{\bullet}OC(CH_3)_3] \rightarrow [(1)Fe^{IV}(X)(OH)\ CH_3{}^{\bullet}\ O{=}C(CH_3)_2] \quad (3)$$

$$[(1)Fe^{IV}(X)(OH)\ CH_3{}^{\bullet}\ O{=}C(CH_3)_2] \rightarrow (1)Fe^{III}(X)(H_2O) + CH_3OH + O{=}C(CH_3)_2$$

(8) Hill, H. A. O.; Thornalley, P. J. *Inorg. Chim. Acta* **1982**, *67*, L35.

$$(1)Fe^{IV}(O)(X) + ABTS \rightarrow (1)Fe^{III}(H_2O)(X) + ABTS^{\bullet+} \quad (4)$$

$$t\text{-}BuO^{\bullet} + ABTS + H^{+} \rightarrow t\text{-}BuOH + ABTS^{\bullet+} \quad (5)$$

fragmentation of t-BuO$^{\bullet}$ to provide $(CH_3)_2CO$ and $CH_3^{\bullet}$ in aqueous solution is known to be 1.4×10^6 s^{-1}.[9]

The lack of formation of $(t\text{-BuO})_2$ establishes that the reactions of eq 6 and 7 are of little consequence in the present study. The

$$2t\text{-}BuO^{\bullet} \rightarrow (t\text{-}BuO)_2 \quad (6)$$

$$2t\text{-}BuOO^{\bullet} \rightarrow (t\text{-}BuOO)_2 \rightarrow (t\text{-}BuO)_2 + O_2 \quad (7)$$

dimerization of t-BuO$^{\bullet}$ (eq 6) (10^9 M^{-1} s^{-1})[10] competes with its fragmentation (1.4×10^6 s^{-1})[9]. However, because of the low concentration of t-BuO$^{\bullet}$, the bimolecular reaction of eq 6 is *disfavored* when compared to the unimolecular fragmentation of t-BuO$^{\bullet}$. Thus, the concentration of t-BuO$^{\bullet}$, at any time, cannot exceed the initial concentration of $(1)Fe^{III}(X)(H_2O)$ (4.6×10^{-6} M) so that the fragmentation reaction is favored over dimerization (eq 6) by a minimal 230-fold. Some t-BuOO$^{\bullet}$ is detectable by EPR when using DMPO as a spin trap. The most likely source of t-BuOO$^{\bullet}$ radicals would seem to be from the reaction of $(1)Fe^{IV}(OH)(X)$ with t-BuOOH (eq 8). We have[11] previously

$$(1)Fe^{IV}(OH)(X) + t\text{-}BuOOH \rightarrow (1)Fe^{III}(H_2O)(X) + t\text{-}BuOO^{\bullet} \quad (8)$$

observed the formation of $(t\text{-BuO})_2$ in neat CH_2Cl_2 on reaction of t-BuOOH with $(TPP)Mn^{III}(X)$ and proposed the mechanism of eq 9. Traylor and Xu[12] subsequently reported the formation

$$(TPP)Mn^{V}(O)(ImH) + t\text{-}BuOOH \rightarrow (TPP)Mn^{IV}(OH)(ImH) + t\text{-}BuOO^{\bullet} \quad (9)$$

$$2t\text{-}BuOO^{\bullet} \rightarrow (t\text{-}BuOO)_2 \rightarrow O_2 + (t\text{-}BuO)_2$$

of $(t\text{-BuO})_2$ in the reaction of $(Cl_8TPP)Fe^{III}(Cl)$ with C_6F_5IO in the presence of t-BuOOH in the solvent mixture CH_2Cl_2/MeOH/H_2O [80/18/2 (v/v)]. They suggested a like mechanism (eq 10).

$$(^{+\bullet}Cl_8TPP)Fe^{IV}(O)(X) + t\text{-}BuOOH \rightarrow (Cl_8TPP)Fe^{IV}(OH)(X) + t\text{-}BuOO^{\bullet} \quad (10)$$

$$2t\text{-}BuOO^{\bullet} \rightarrow (t\text{-}BuOO)_2 \rightarrow O_2 + (t\text{-}BuO)_2$$

For the reaction of t-BuOOH with $(1)Fe^{III}(X)(H_2O)$ (Results), plots of the log of the second-order rate constant (k_{ly}) vs pH (2–13) provide a complex profile which may be fitted by the same empirical equation (eq 2) employed to fit the experimental data when employing ABTS as a trap for both $(1)Fe^{IV}(O)(X)$ and t-BuO$^{\bullet}$.[1] An interpretation of the log k_{ly} vs pH profile in terms of reaction steps has been presented[1] in the study that employed ABTS as a trap. The sequence of proposed reactions is presented in Scheme I, which also shows the relationship of the empirical rate and pK_{app} values to the true kinetic constants and actual pK_a values. The empirical rate constants and pK_{app} values of this study are compared to those determined with ABTS present in Table I. This comparison shows that the rate constants are 2-3-fold greater in the absence of ABTS. This may be explained as follows. In the presence of ABTS one is following the formation of both $(1)Fe^{IV}(O)(X)$ and t-BuO$^{\bullet}$ (eq 4 and 5), while in the absence of ABTS the disappearance of $(1)Fe^{III}(X)(H_2O)$ is followed. This should provide a difference of 2 in the rate constants. In the absence of ABTS, the reactions are biphasic due to the accumulation of an intermediate. The apparent second-order rate constant, k_{ly}, was determined from $k_{obsd}/[(1)Fe^{III}(X)(H_2O)]$,

Scheme II

$(1)Fe^{III}(X)(t\text{-}BuOO^{-}) \rightarrow [(1)Fe^{IV}(X)(OH)\ {}^{\bullet}OC(CH_3)_3]$
$[(1)Fe^{IV}(X)(OH)\ {}^{\bullet}OC(CH_3)_3] \rightarrow [(1)Fe^{IV}(X)(OH)\ CH_3^{\bullet}\ O{=}C(CH_3)_2]$
$[(1)Fe^{IV}(X)(OH)\ CH_3^{\bullet}\ O{=}C(CH_3)_2] \rightarrow (1)Fe^{III}(X) + CH_3OH + O{=}C(CH_3)_2$
$(1)Fe^{III}(X)(t\text{-}BuOO^{-}) \rightarrow (1)Fe^{IV}(OH)(X) + (CH_3)_3CO^{\bullet}$
$(CH_3)_3CO^{\bullet} \rightarrow CH_3^{\bullet} + (CH_3)_3C{=}O$
$(1)Fe^{IV}(X)(OH) + CH_3^{\bullet} \rightarrow (1)Fe^{III}(X)(H_2O) + CH_3OH$
$(1)Fe^{III}(X)(H_2O) + CH_3^{\bullet} \rightarrow (1)Fe^{II}(X)(H_2O) + CH_3OH$
$(1)Fe^{II}(X)(H_2O) + O_2 \rightarrow (1)Fe^{III}(X)O_2^{\bullet-}$
$(1)Fe^{II}(X)(H_2O) + (1)Fe^{III}(X)O_2^{\bullet-} \rightarrow (1)(X)Fe^{III}O\text{–}OFe^{III}(X)(1)$
$(1)(X)Fe^{III}O\text{–}OFe^{III}(X)(1) \rightarrow 2(1)Fe^{IV}(O)(X)$
$(1)Fe^{IV}(OH)(X) + (CH_3)_3COOH \rightarrow (1)Fe^{III}(OH)(X) + (CH_3)_3COO^{\bullet} + H^{+}$
$(CH_3)_3COO^{\bullet} \rightarrow (CH_3)_3CO^{\bullet} + {}^1/_2O_2$
$(CH_3)_3CO^{\bullet} \rightarrow (CH_3)_2C{=}O + CH_3^{\bullet}$
$(1)Fe^{IV}(OH)(X) + CH_3^{\bullet} + H_2O \rightarrow (1)Fe^{III}(H_2O)(X) + CH_3OH$

where k_{obsd} is the pseudo-first-order rate constant for the initial phase. Since k_{obsd}, so determined, shows a linear dependence upon $[t\text{-BuOOH}]_i$ this procedure is akin to the use of initial rates. Of the four kinetically apparent pK_{app} values three are quite similar. The values of pK_C differ by 1.6 units. This divergence may be more apparent than real since, in the absence of ABTS, it was determined from only two points. The unescapable conclusion is that the shape of the profile (i.e., similarity of rate and kinetically apparent acid dissociation constants; Table I) fingerprints the values of k_{ly} as belonging to the same rate-determining steps in the presence or absence of ABTS.

Between pH 5 and 7 There Is Seen To Be Formed Iron(IV)–Oxo Porphyrin Intermediates. The spectrum of the intermediate formed at pH 6.70 (Figure 2) differs from that formed at pH 5.14 (Figure 3). Titration of the product formed at pH 5.14 with ABTS shows that it is 1e- oxidized above the iron(III) state. Interestingly, the spectrum of the product seen at pH 5.14 compares favorably with the electrochemically generated $(Me_{12}TPP)Fe^{IV}(O)$ species in CH_2Cl_2.[13] The half-wave potentials for the 1e- oxidation of $(1)Fe^{III}(X)(H_2O)$ at pH 5.14 and 6.7 in water were determined at a carbon microelectrode by linear sweep voltammetry as 0.86 and 0.81 V (SCE), respectively. The iron(IV) species was generated by electrochemical oxidation of $(1)Fe^{III}(X)(H_2O)$ at pH 6.72 and found to be essentially identical with that of the intermediate generated by the oxidation of $(1)Fe^{III}(X)(H_2O)$ with alkyl hydroperoxides and MCPBA at this pH.

The influence of oxygen on the formation of an iron(IV)-oxo porphyrin intermediate in the reactions of $(1)Fe^{III}(X)(H_2O)$ with the hydroperoxides $Ph_2C(CN)OOH$, $Ph_2C(CO_2CH_3)OOH$, $PhC(CH_3)_2OOH$, $(CH_3)_3COOH$, and m-chloroperbenzoic acid (MCPBA) is crucial to the definition of mechanism. Our observations that iron(IV)–oxo porphyrin intermediates are formed with alkyl hydroperoxide between pH 5 and 7 only in the presence of O_2 are strongly suggestive of the intermediacy of an iron(II) porphyrin species. On the other hand, the formation of an iron(IV)–oxo porphyrin intermediate on reaction of MCPBA with $(1)Fe^{III}(X)(H_2O)$ in the presence or absence of O_2 is in accord with 2e- oxidation of $(1)Fe^{III}(X)(H_2O)$ followed by a comproportionation reaction (eq 11). Thus, in the formation of an

$$(1)Fe^{III}(X)(H_2O) + m\text{-}ClC_6H_4CO_3H \rightarrow (^{+\bullet}1)Fe^{IV}(O)(X) + m\text{-}ClC_6H_4CO_2H$$

$$(1)Fe^{III}(X)(H_2O) + (^{+\bullet}1)Fe^{IV}(O)(X) \rightarrow 2(1)Fe^{IV}(O)(X) + 2H^{+} \quad (11)$$

iron(IV)–oxo porphyrin in the percarboxylic acid reaction, the first step involves heterolytic cleavage of the percarboxylic acid O–O bond.[2,14] In the reaction of alkyl hydroperoxides with

(9) Erben-Russ, M.; Michael, C.; Bors, W.; Saran, M. *J. Phys. Chem.* **1987**, *91*, 2362.
(10) Niki, E.; Kamiya, Y. *J. Am. Chem. Soc.* **1974**, *96*, 2129.
(11) Balasubramanian P. N.; Sinha, A.; Bruice, T. C. *J. Am. Chem. Soc.* **1987**, *109*, 1456.
(12) Traylor, T. G.; Xu, F. *J. Am. Chem. Soc.* **1987**, *109*, 6201.
(13) (a) Calderwood, T. S.; Bruice, T. C. *Inorg. Chem.* **1986**, *25*, 3722. (b) Calderwood, T. S.; Lee, W. A.; Bruice, T. C. *J. Am. Chem. Soc.* **1985**, *107*, 8272. (c) Lee, W. A.; Calderwood, T. S.; Bruice, T. C. *Proc. Natl. Acad. Sci. U.S.A.* **1985**, *82*, 4301.

Scheme III

$$(\mathbf{1})Fe^{III}(X)(H_2O) + (CH_3)_3COOH \rightarrow (\mathbf{1})Fe^{II}(X)(H_2O) + (CH_3)_3COO^{\bullet} + H^+$$
$$2(CH_3)_3COO^{\bullet} \rightarrow 2(CH_3)_3CO^{\bullet} + O_2$$
$$(\mathbf{1})Fe^{II}(X)(H_2O) + O_2 \rightarrow (\mathbf{1})Fe^{III}(X)(O_2^{\bullet-})$$
$$(\mathbf{1})Fe^{II}(X)(H_2O) + (\mathbf{1})Fe^{III}(X)(O_2^{\bullet-}) \rightarrow [(\mathbf{1})Fe^{III}(X)O]_2$$
$$[(\mathbf{1})Fe^{III}(X)O]_2 \rightarrow 2(\mathbf{1})Fe^{IV}(O)(X)$$
$$(CH_3)_3CO^{\bullet} \rightarrow CH_3^{\bullet} + (CH_3)_2C{=}O$$
$$(\mathbf{1})Fe^{III}(X)(H_2O) + CH_3^{\bullet} \rightarrow (\mathbf{1})Fe^{II}(X)(H_2O) + CH_3OH$$
$$(\mathbf{1})Fe^{IV}(O)(X) + CH_3^{\bullet} \rightarrow (\mathbf{1})Fe^{III}(X)(H_2O) + CH_3OH$$

$(\mathbf{1})Fe^{III}(H_2O)(X)$, the iron(IV)–oxo porphyrin must arise via a homolytic scission. With cumyl hydroperoxide, product analysis has established the intermediate formation of $Ph(CH_3)_2CO^{\bullet}$.[1]

The mechanism of the reaction of *t*-BuOOH with $(\mathbf{1})Fe^{III}(X)(H_2O)$ may be discussed in terms of Scheme II and by consideration of the kinetically equivalent Scheme III. The kinetic dependence upon pH for the reaction of *t*-BuOOH with $(\mathbf{1})Fe^{III}(X)(H_2O)$ establishes the presence of four distinct pathways (Scheme I). The following discussion pertains mainly to the pH region of 5–7 where the formation of $(\mathbf{1})Fe^{IV}(OH)(X)$ is observed. The first three reactions of Scheme II represent the caged reactions where intermediates cannot be trapped by ABTS (eq 3). The overall reaction of Scheme II is given in eq 12. The rate constant (2.3×10^9 M^{-1} s^{-1}) for the reaction of $CH_3^{\bullet}$ radical with $(Porph)Fe^{III}(X)$ is known.[15]

$$4(\mathbf{1})Fe^{III}(X)(H_2O) + 4(CH_3)_3COOH + O_2 \rightarrow 4(\mathbf{1})Fe^{IV}(O)(X) + 4(CH_3)_2C{=}O + 4CH_3OH \quad (12)$$

In the reaction of *t*-BuOOH with $(\mathbf{1})Fe^{III}(X)$, $(\mathbf{1})Fe^{IV}(O)(X)$ does not accumulate in the absence of O_2. Under anaerobic conditions, $(\mathbf{1})Fe^{II}(X)(H_2O)$ would be consumed by a comproportionation reaction with $(\mathbf{1})Fe^{IV}(O)(X)$ (eq 13).

$$(\mathbf{1})Fe^{III}(OH)(X) + (CH_3)_3COOH \rightarrow (\mathbf{1})Fe^{IV}(O)(X) + (CH_3)_2C{=}O + CH_3^{\bullet}$$
$$(\mathbf{1})Fe^{III}(OH)(X) + CH_3^{\bullet} \rightarrow (\mathbf{1})Fe^{II}(OH)(X) + CH_3OH \quad (13)$$
$$(\mathbf{1})Fe^{IV}(O)(X) + (\mathbf{1})Fe^{II}(OH)(X) \rightarrow 2(\mathbf{1})Fe^{III}(OH)(X)$$

If the mechanism were to follow that shown in Scheme III then $(\mathbf{1})Fe^{IV}(O)(X)$ should form under anaerobic conditions. This is not seen.

Scheme II predicts the formation of $(\mathbf{1})Fe^{II}(OH)(X)$ as a secondary product. The formation of $(\mathbf{1})Fe^{II}(H_2O)(X)$ (in but ~10% yield based on $[(\mathbf{1})Fe^{III}(X)(H_2O)]_i$) was shown by its trapping with carbon monoxide as $(\mathbf{1})Fe^{II}(H_2O)(CO)$. The identity of $(\mathbf{1})Fe^{II}(H_2O)(CO)$ was established by comparison of spectra to an authentically prepared solution of the latter. It is known that the formation of CO adducts of iron(II) porphyrins is exceedingly rapid ($>10^6$ M^{-1} s^{-1}).[6] The observation of only ~10% of $(\mathbf{1})Fe^{II}(H_2O)(CO)$ adduct is likely due to the comproportionation reaction of $(\mathbf{1})Fe^{IV}(O)(X)$ with $(\mathbf{1})Fe^{II}(H_2O)(CO)$ (eq 14). It may further be stated that if the $(\mathbf{1})Fe^{II}(X)(H_2O)$

$$(\mathbf{1})Fe^{II}(X)(CO) + (\mathbf{1})Fe^{IV}(O)(X) + H_2O \rightarrow 2(\mathbf{1})Fe^{III}(X)(H_2O) + CO \quad (14)$$

species is generated by Fenton chemistry (Scheme III), then one would be able to trap greater than 90% of $(\mathbf{1})Fe^{II}(H_2O)(X)$ if the rate constant for the formation of $(\mathbf{1})Fe^{II}(X)(CO)$ (eq 15a) is greater than the rate constant for the reaction of $(\mathbf{1})Fe^{II}(X)(H_2O)$ with $(CH_3)_3COOH$ (eq 15b).

$$(\mathbf{1})Fe^{II}(X)(H_2O) + CO \rightarrow (\mathbf{1})Fe^{II}(X)(CO) \quad (15a)$$
$$(\mathbf{1})Fe^{II}(X)(H_2O) + (CH_3)_3COOH \rightarrow (\mathbf{1})Fe^{III}(OH)(X) + CH_3CO^{\bullet} \quad (15b)$$

The intermediates that are subject to trapping by ABTS arise from 1e- transfer from $(\mathbf{1})Fe^{III}(X)(H_2O)$ to the hydroperoxide. From a comprehensive kinetic investigation[1] the commitment electron-transfer step occurs within the complexes $(\mathbf{1})Fe^{III}(X)$-(*t*-BuOOH) and $(\mathbf{1})Fe^{III}(X)(t\text{-}BuOO^-)$ to provide *t*-$BuO^{\bullet}$ and $(\mathbf{1})Fe^{IV}(O)(X)$ species (Scheme II). Fragmentation of *t*-$BuO^{\bullet}$ provides $CH_3^{\bullet}$ and, in a minor reaction, oxidation of *t*-BuOOH by $(\mathbf{1})Fe^{IV}(O)(X)$ gives *t*-$BuOO^{\bullet}$. The time course of formation of the *t*-$BuOO^{\bullet}$, *t*-$BuO^{\bullet}$, and $CH_3^{\bullet}$ spin-trapped adducts of 5,5-dimethyl-1-pyrroline *N*-oxide (DMPO) have been followed. Formation of $(t\text{-}BuO)_2$ is not seen. As explained in Results (see discussion concerning eq 6 and 7), dimerization of *t*-$BuO^{\bullet}$ cannot compete with its fragmentation. Further, in the self-reaction of *t*-$BuOO^{\bullet}$, breakdown of the caged intermdiates (eq 16) in organic solvents provides mainly *t*-$BuO^{\bullet}$ rather than $(t\text{-}BuO)_2$.[16] Perhaps the formation of *t*-$BuO^{\bullet}$ is the only path in water.

$$2t\text{-}BuOO^{\bullet} \rightarrow [t\text{-}BuO^{\bullet}\ O_2\ {}^{\bullet}OBu\text{-}t] \quad (16)$$
$$[t\text{-}BuO^{\bullet}\ O_2\ {}^{\bullet}OBu\text{-}t] \rightarrow 2t\text{-}BuO^{\bullet} + O_2$$
$$[t\text{-}BuO^{\bullet}\ O_2\ {}^{\bullet}OBu\text{-}t] \rightarrow (t\text{-}BuO)_2 + O_2$$

Scheme II explains the following observations: (i) The generation of iron(IV) oxo intermediate species, only in the presence of O_2, on reaction of alkyl hydroperoxides (*t*-BuOOH and $(CH_3)_2C(Ph)OOH$) is due to the reaction of intermediate iron(II) porphyrin with O_2. The iron(II) porphyrin is formed by rebound reduction of $(\mathbf{1})Fe^{III}(X)(H_2O)$ by carbon-centered radicals produced in the fragmentation of alkoxy radicals.[15] (ii) The lag phase seen at small excess of *t*-BuOOH is due to competitive reactions of $(\mathbf{1})Fe^{IV}(OH)(X)$ with $CH_3^{\bullet}$[15] and *t*-BuOOH.[11] (iii) The spin-trapping experiments support the formation of *t*-$BuOO^{\bullet}$, *t*-$BuO^{\bullet}$, and $CH_3^{\bullet}$ radicals. The lack of knowledge of the efficiency of trapping of radical species by DMPO as well as a lack of understanding as to whether increase in pH affect *t*-$BuOO^{\bullet}$ stability or the stability of the adduct of *t*-$BuOO^{\bullet}$ prohibits quantitative analysis of absolute radical concentrations. (iv) In the absence of O_2, $(\mathbf{1})Fe^{II}(X)(H_2O)$ disappears from solution by comproportionation reaction with $(\mathbf{1})Fe^{IV}(OH)(X)$. It seems likely that the reaction of $(\mathbf{1})Fe^{IV}(OH)(X)$ with *t*-BuOOH to generate *t*-$BuOO^{\bullet}$ species and the subsequent formation of O_2 can amount to only an insignificant fraction of the reaction.

Hydrogen peroxide appears to be a special case. A $(\mathbf{1})Fe^{IV}(OH)(X)$ species does not accumulate on reaction of H_2O_2 with $(\mathbf{1})Fe^{III}(X)(H_2O)$. Also, it has been shown (Results) that the intermediate iron(IV) porphyrin species (Soret at 421 nm) generated with *t*-BuOOH disappears rapidly on addition of hydrogen peroxide. These are interesting observations, since it establishes the reactivity of H_2O_2 with an iron(IV) oxo porphyrin (presumably as in eq 17).

$$(\mathbf{1})Fe^{IV}(X)(H_2O) + HOOH \rightarrow (\mathbf{1})Fe^{III}(X)(H_2O) + HO_2^{\bullet} + H^+ \quad (17)$$
$$HO_2^{\bullet} \rightleftarrows H^+ + O_2^{\bullet-} \qquad (pK_a\ 4.6)$$
$$2HO_2^{\bullet} \rightarrow HOOH + O_2$$

Acknowledgment. This work was supported by the National Institutes of Health and the National Science Foundation. J. R.L.S. thanks the SERC (UK) for travel funds to visit and carry out research at U.C.—Santa Barbara.

(14) (a) Traylor, T. G.; Lee, W. A.; Stynes, D. V. *J. Am. Chem. Soc.* **1984**, *106*, 755. (b) Traylor, T. G.; Lee, W. A.; Stynes, D. V. *Tetrahedron* **1984**, *40*, 553.

(15) Brault, D.; Neta, P. *J. Am. Chem. Soc.* **1981**, *103*, 2705.

(16) (a) Ingold, K. U. In *Free Radicals*, Kochi J. K., Ed.; John Wiley and Sons: New York, 1973; Vol. I, Chapter 2. (b) Howard, J. A. In *Advances in Free Radical Chemistry*; Williams, G. H., Ed.; Academic Press: New York, 1972; Vol. 4, Chapter 2.